Polyp Segmentation Method
for CT Colonography Computer Aided Detection

Anna K. Jerebko[1] [a,b], Sheldon B. Teerlink[c], Marek Franaszek[a], Ronald M. Summers[a]

[a]Diagnostic Radiology Department, National Institutes of Health, Bethesda, MD 20892-1182
[b]Current address: Siemens Medical Solutions USA, Inc., Malvern, PA 19355
[c]Utah State Univ., Logan UT 84321

ABSTRACT

We have developed a new method employing the Canny edge detector and Radon transformation to segment images of polyp candidates for CT colonography (CTC) computer aided polyp detection and obtain features useful for distinguishing true polyps from false positive detections.
The technique is applied to two-dimensional subimages of polyp candidates selected using various 3-D shape and curvature characteristics. We detect boundaries using the Canny operator. The baseline of the colon wall is detected by applying the Radon transform to the edge image and locating the strongest peak in the resulting transform matrix. The following features are calculated and used to classify detections as true positives (TP) and false positives (FP): polyp boundary length, polyp base length, polyp internal area, average intensity, polyp height, and inscribed circle radius. The segmentation technique was applied to a data set of 15 polyps larger than 3 mm and 617 false positives taken from 80 CTC studies (supine and prone screening of 40 patients). The sensitivity was 100% (15 of 15). 58% of the FP's were eliminated leaving an average of 3 false positives per study.
Our method is able to segment polyps and quantitatively measure polyp features independently of orientation and shape.

Keywords: CT colonography, virtual colonoscopy, polyp, segmentation, Canny filter.

1. INTRODUCTION

Colon cancer is the second leading cause of cancer death in America [1]. For years people have undergone colonoscopies, which are the gold standard for examining the condition of the colon. In preparation for the colonoscopy, a patient goes through several steps that may include a 48 hour liquid diet, a milk of magnesia drink, laxative or an enema. The patient is then some what sedated as an endoscope travels past the rectum and through the colon. If small polyps are discovered they are removed by a tool on the end of the endoscope. Large polyps must be removed surgically. The danger these polyps present, if left to grow, is the potential to become cancerous. Both malignant and benign cases have been reported [2]. Often circumstances will prevent a complete and accurate colonoscopy from being performed or introduce additional complications. A sharp bend or twist in the colon will prevent the endoscope from passing the entire length, leaving certain regions indeterminate. With older patients there is the risk of puncturing the colon wall, causing bleeding and further discomfort. Polyps of the colon and rectum occur in more than 25% of the U.S. population over 50 years of age [3]. In hopes of alleviating many of the risks and pain as well as reduce the costs of colonoscopies a new method, CT colonography (CTC), is being researched.

A CTC examination consists of a CT scan of the abdomen, obtaining between 100 – 500 2D images (supine and prone). To obtain the CT images the colon is distended by pumping a small amount of air into the colon through the rectum using a rectal tube. The scan time for each patient is only 3 -5 minutes with no anesthetic involved. A radiologist will have to evaluate each image and identify any polyps that may exist. Computer aided detection is important in CTC because the interpretation time for each patient is 15-20 minutes and it may help to identify the polyps even experienced radiologists can miss due to fatigue or perceptual errors. Using computer aided-detection (CAD) those images with areas of high curvature and sphericity are segmented and classified as polyp or non polyp [4]. Applying CAD to CTC may improve interpretation results and is more attractive both in physical comfort and cost.

---

[1] anna.jerebko@siemens.com

Polyps fall into three general categories: sessile, pedunculated, and flat. It is important to detect polyps independently of a specific shape category, orientation, or size. Images of the three types of polyps appear in figure 1. Flat polyps are the most difficult to detect, but they could be detected if they have elevation compared to surrounding colon wall such as the polyps in Figure 1 (b). Sessile polyps are attached directly to the colon wall usually with a broad base and pseudopedicle. Pedunculated polyps may be attached to the colon with a pedicle that may be thin, thick, short, or long. Hyperplastic polyps are small sessile mucosal elevations of the colon and rectum with a distinctive histologic appearance. Other methods to segment the polyp have not found great success unless the polyp possesses certain specific characteristics. Gokturk et al. relies entirely on the fact that polyps can be fit by a circle, quadratic, or line to the largest connected edge component [5]. For nicely shaped polyps this method can work but many polyp images may have non-circular shape (as polyps in the figure 1), contain weak edges and noise. The resulting edge detection leaves gaps and has missing contours especially when using the Sobel operator proposed in [5]. When trying to fit a window to a suspicious structure they exclude as much of the extraneous tissue as possible. This can lead to higher detections of stool and an increase in false positives because the polyp attachment to the colon wall is not considered.

We have developed a new computer aided diagnostic technique to segment the colon wall, forming the candidate lesion and then classify individual images as polyp or non-polyp. The algorithm is based on finding structures elevated compared to surrounding colon wall. As one step of our algorithm we also employ a circle fitting procedure. We use it together with the polyp base line and intensity threshold to determine the polyp inside area not relying on the full connectedness of the polyp edge. Using this method virtually any polyp can be segmented if it is not completely flat and has no rise compared to the surrounding colon wall. Our algorithm is able to quantitatively measure particular features (polyp boundary length, number of boundary pixels, polyp base length, polyp internal area, mean intensity, polyp height, and inscribed circle radius) of the polyp and use them for classification. Our approach allows to measure these features independently of polyp orientation and shape. The proposed algorithm it is very simple to code and implement. Using this method we have been able to achieve high sensitivity while reducing the number of false positive detections and diagnosis time.
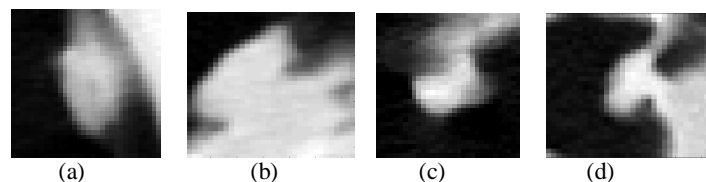

| | | | |
| (a) | (b) | (c) | (d) |

Figure 1. (a) Sessile polyp. (b) Sessile polyp with a flat top. (c)-(d) Pedunculated polyps.

2. METHODS

Here is a brief description of our methods followed by finer details and explanations. Each polyp candidate image our algorithm processes is generated from regions of the colon within certain thresholds for curvature and sphericity. The number of images processed represents approximately 5% of the colon [4]. Many of these images are not polyps but rather folds in the colon wall, leftover stool, or some other anatomical structure. Even the tip of the rectal tube used to pump air into the colon during the CT scan will be detected because of its smooth round surface (Figure 2). Often the rectal tube is pressed against the colon wall and is more difficult to distinguish than rectal tubes surrounded completely by lumen. A few of these images are legitimate polyps. The goal is to separate the true polyps from the larger group of polyp candidates.

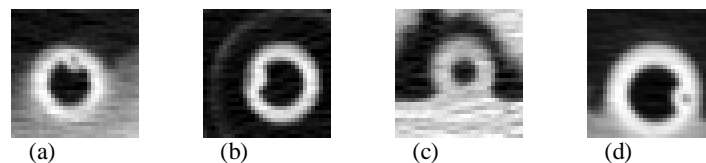| | | | |
| (a) | (b) | (c) | (d) |

Figure 2. (a)-(d) Images of rectal tubes acquired during the CT scan are detected and identified as false positives

We begin by applying a median filter to the image to reduce noise. Next we use an edge detector to identify polyp boundaries. From here we locate the baseline of the colon wall by applying the Radon transform and selecting the strongest point in the transform matrix. The theta value corresponding to the strongest point in the transform matrix is used to rotate the original image and contour image to lie horizontally along the polyp baseline. The junction of the polyp with the colon wall is located by finding a chord between the two outermost contour points which only pass through soft tissue but not lumen. The chord approximates the polyp baseline. Polyp wall points are linked by locating chords parallel to the base. Bisecting these chords yields a centerline through the polyp. These baseline and height measurements are used to inscribe a circle about the region of interest and to compute the radius of the circle. From here the polyp arc length and the number of pixels on the polyp boundary are found using circle geometry. Lastly the polyp area is calculated in conjunction with the mean intensity of the identified polyp. From this process seven unique features are obtained to classify the segmented image as polyp or non-polyp.

2.1. Edge Detection

Our first step is to reduce noise in the image without introducing new image pixel values and blurring edges. This is done by applying a 3x3 median filter over the entire image before we begin detecting edges. Edge detection is very important because the strength of our algorithm lies in processing the resulting contour image. Some of the common edge detectors include Sobel, Roberts Cross, and Prewitt [6,7,8,9]. These edge operators detect the gradient of an image $f(x,y)$ at each location (x,y) in the image. The gradient is represented by the vector

$$\nabla f = \begin{bmatrix} Gx \\ Gy \end{bmatrix} = \begin{bmatrix} \dfrac{\partial f}{\partial x} \\ \dfrac{\partial f}{\partial y} \end{bmatrix} \tag{1}$$

which points in the direction of the maximum rate of change in the image f at the location (x,y). The magnitude of the vector (1)

$$mag(\nabla f) = \left[\left(\frac{\partial f}{\partial x} \right)^2 + \left(\frac{\partial f}{\partial y} \right)^2 \right]^{1/2} \tag{2}$$

is the method these edge detectors use for image differentiation. In the spatial domain a kernel is convolved with the 2D image to detect the gradients in the image. Sobel and Prewitt use two 3x3 kernels. One kernel is applied to detect the gradient in the x direction while the other kernel is applied to detect the gradient in the y direction. Roberts Cross uses two kernels of size 2x2 to detect the cross differences.

Although these detectors are simple to understand and implement they posses a number of drawbacks such as thick edges, and segmented edges when the true edge is really continuous. For these reasons we choose to use the Canny edge detector [10]. The Canny algorithm still uses the gradient method to detect change in magnitude but it also uses non-maximal suppression and hysteresis tracking to recover "weak" edges if they are connected to strong ones and to produce thin edges. The Canny edge detector works in a multistage process. First of all the image is smoothed by Gaussian convolution based on the parameter σ between 0.6 and 4.0. The Gaussian distribution is given by

$$G(x, y) = \frac{1}{2\pi\sigma^2} e^{\frac{-x^2+y^2}{2\sigma^2}} \tag{3}$$

Then a simple 2-D first derivative operator is applied to the smoothed image to highlight regions of the image with high first spatial derivatives in the direction of the gradient *n*.

$$n = \frac{\nabla(G * f)}{\left|\nabla(G * f)\right|} \tag{4}$$

Edges give rise to ridges in the gradient magnitude image and can be detected by tracking along the top of these ridges and setting to zero all pixels that are not actually on the ridge top so as to give a thin line in the output. This process is known as *non-maximal suppression*. The tracking process exhibits hysteresis controlled by two thresholds: *T-high* and *T-low*, with *T-high* > *T-low*. Tracking can only begin at a point on a ridge higher than *T-high*. Tracking then continues in both directions out from that point until the height of the ridge falls below *T-low*. This hysteresis helps to ensure that noisy edges are not broken up into multiple edge fragments. Figure 3 shows the results of applying various edge detectors to polyp candidates.
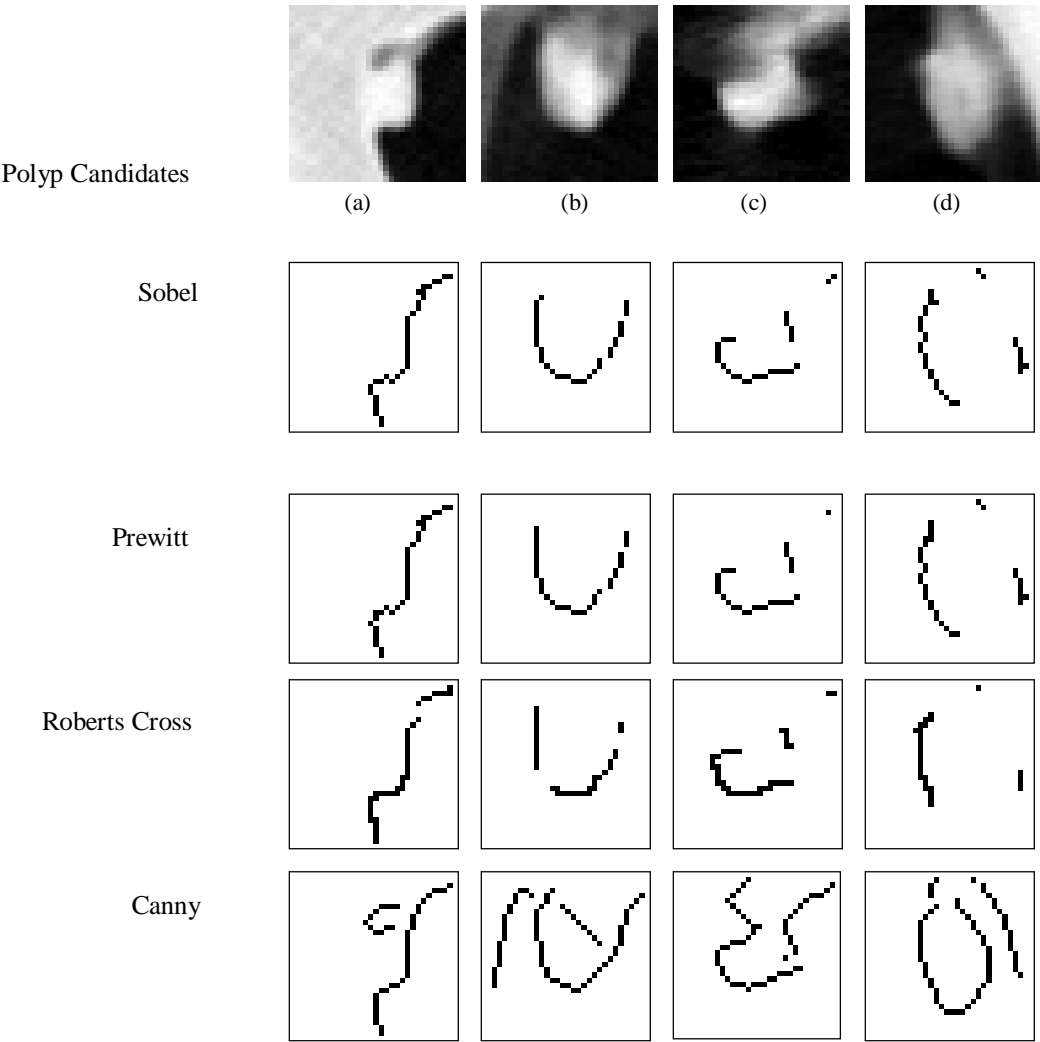
Figure 3. (a) Sessile polyp, (b) hanging polyp, (c) pedunculated polyp, (d) polyp with weak edges.

It appears the Sobel operator, which is used by a group of scientists at Stanford for polyp segmentation, and the Prewitt edge operator, produce the same contour images [5]. This is because other than Sobel's slight smoothing effects, the kernels for both operators are identical. The Sobel operator produces an incomplete contour image and is not suitable for segmenting all kinds of real polyps. Roberts Cross performs poorly for our purposes as can be seen by the number of line gaps and thicker edges. Polyp candidate (b) is a good example of how a "weak" edge, which in this case is the colon wall, can be detected if it is attached to a strong edge using the Canny algorithm. For each of the polyp candidates Sobel, Prewitt, or Roberts Cross did not create an acceptable contour image for further segmentation.

Other edge detectors using models require a priori knowledge of the polyp shape which may not work with all varieties of polyp shapes. Despite this fact we admit the Canny edge detector can be substituted with deformable models or snakes for this step of the algorithm as long as it produces thin connected edges and segments the polyp with the surrounding colon wall.

2.2. Colon Wall Detection

After applying the Canny filter, the Radon transformation (which is closely related to the Hough transformation) is applied to the contour image. The Radon transform computes projections in the contour image $c(x,y)$ along specified directions. In general, projections can be computed along any angle θ using the line integral [11,12]

$$R_\theta(x') = \int_{-\infty}^{\infty} (x'\cos\theta - y'\sin\theta, x'\sin\theta + y'\cos\theta)dy' \qquad (5)$$

and

$$\begin{bmatrix} x' \\ y' \end{bmatrix} = \begin{bmatrix} \cos\theta & \sin\theta \\ -\sin\theta & \cos\theta \end{bmatrix} \begin{bmatrix} x \\ y \end{bmatrix} \qquad (6)$$

into the (ρ, θ) domain (see example in the figure 4). For our purposes we compute the angles of projection from 0 to 180 degrees. The points with highest intensity in the (ρ, θ) domain correspond to the longest lines in the (x,y) plane. We are only concerned with the theta value corresponding to the highest intensity θ_{Imax} in the (ρ, θ) domain because in nearly every case the longest line corresponds to the colon wall. Locating the colon wall is important because it allows us to rotate the polyp image to a standard position for further processing. The angle of rotation is equal to 90 - θ_{Imax}
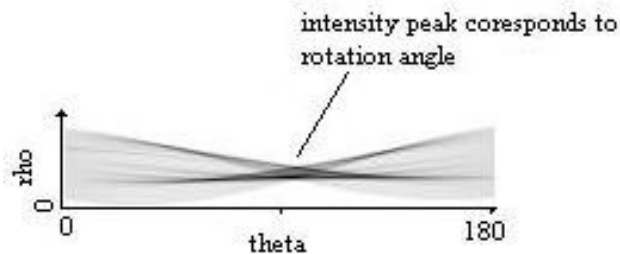

Figure 4. Radon transformation from $\theta=0° – 180°$ of a particular sessile polyp shows high intensity regions close to the center which corresponds to $\theta_{Imax} = 90°$. In this case $\theta_{Imax} = 96°$ so the original and contour images are rotated 6°.

Both the original image and the contour image are rotated so the colon wall lies horizontally and the polyp either floats upward or hangs beneath (figure 5). Because a myriad of polyp orientations exist, the Radon transformation allows us to eliminate the need to process the polyp in several different positions. Only two positions need to be considered, one with the polyp above the colon wall and one where the polyp hangs beneath.
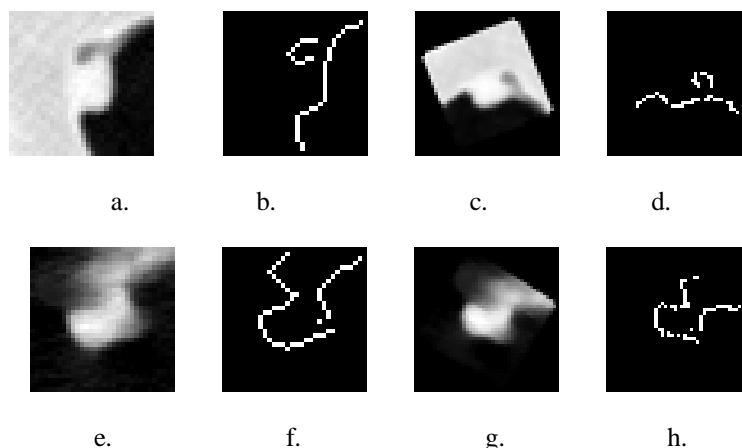

Figure 5. (a),(e) Polyp candidates in original position. (b),(f) Result of Canny edge detector, (c),(g) Polyp candidates rotated. (d),(h) Edge images rotated.

2.3. Polyp Feature Extraction

Now it is possible to begin extracting and measuring polyp features. We begin measuring polyp features by locating the junction between the polyp and the colon wall. To do this we find a chord between the two outermost contour points which pass only through soft tissue but not the colonic lumen. We determine if the line passes only through soft tissue by placing a circular mask in the middle of the chord and calculating the average intensity of all pixels in the mask. If the mean intensity is above a certain threshold and the number of low intensity pixels in the mask is less than the number of high intensity pixels, it is declared as passing only through soft tissue.

In figure 6a, chord 1 passes through the colonic lumen, chord 2 doesn't pass the chord to apex distance requirement, chords 3 and 4 are considered as polyp baselines, and chord 4 is selected because it results in the best fitting inscribed circle. Note that it is not immediately apparent which chord will be selected solely on its proximity to the colon wall. Once a satisfactory chord is found the length of line segment AB becomes the polyp base length.
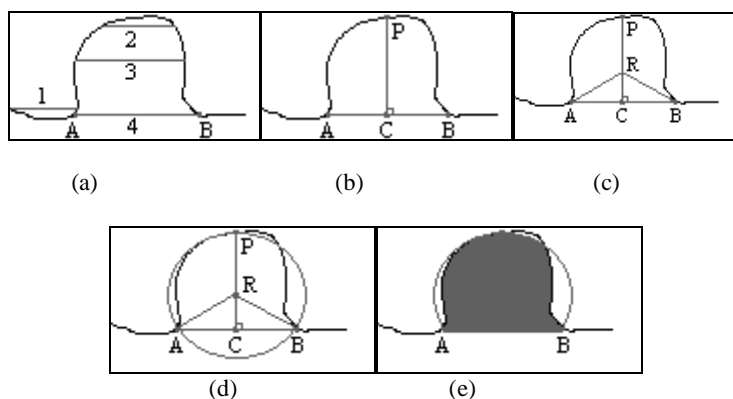

Figure 6. (a)-(e) visual depiction of algorithmic polyp separation.

If the chord (AB) is long enough and passes only through soft tissue, a perpendicular line, beginning at the baseline center and extending to the polyp apex (line segment CP in figure 6b.), is computed as

$$polyp\ height = \left[\left(C_x - P_x\right)^2 + \left(C_y - P_y\right)^2 \right]^{1/2} \tag{7}$$

Once we know the chord length (AB) and the polyp height we can compute the radius of the inscribed circle.

Figure 6c shows point R as the center of the inscribed circle. A circle can be inscribed inside the polyp knowing the chord length and the height. The radius of the circle is calculated using circle geometry and is given by

$$polyp\ radius = \frac{l^2}{8h} + \frac{h}{2} \tag{8}$$

where

$$l = dist(A,B)\ \text{and}\ h = dist(P,\ C) \tag{9}$$

Polyp boundary length is a calculated approximate measurement using l and h and is an approximation of the polyp perimeter.

$$polyp\ boundary\ length \approx \sqrt{l^2 + \frac{16h^2}{3}} \tag{10}$$

In figure 6d the inscribed circle connects points A, B, and P to form arc (APB).

The actual polyp boundary can weave in and out of the inscribed circle as figure 6d shows. When the polyp boundary length is compared to the true polyp boundary length the results are nearly the same. Another measure of the polyp boundary is the number of actual pixels on the arc. This value can be found by measuring the distance d of each pixel from the center of the circle R and testing to see if the following condition is satisfied.

$$|d - r| \le \Delta \tag{11}$$

If a pixel is less than a distance Δ on either side of the inscribed circle it is selected as a polyp boundary pixel. The union of all these pixels is the number of *polyp boundary pixels*.

Now that we've computed the inscribed circle radius, polyp boundary length, and number of contour pixels on the polyp boundary we can estimate the *polyp area p(x,y)*. Each pixel in *p(x,y)* is inside the inscribed circle, has intensity greater than a set threshold and is not outside the bounds of the contour. See figure 6e. Testing the intensity value ensures the pixels selected are not part of the lumen or surrounding colon wall which generally has lower intensity values. To test whether a pixel lies within the ideal intensity range a local average intensity is computed by summing the current pixel's intensity value with the intensity values of the 8 pixel neighbors and dividing by 9. This method is used to determine if a pixel has an intensity value great enough to be a member of *p(x,y)*.

From *p(x,y)* we can simply compute the mean intensity of the polyp by summing all intensity values in *p(x,y)* and divide by N

$$polyp\ mean\ intensity = \frac{\displaystyle\sum_{\forall(x,y)\in p(x,y)} I_{(x,y)}}{N} \qquad (12)$$

where N is the number of pixels in *p(x,y)*.

There are a small number of cases where using this method does not span a horizontal chord within the polyp interior from wall to wall as we discussed in the first step. This occurs when the rotation of the contour image is such that an edge exists on one side of the polyp but not on the other. The example of such a polyp is given in figure 7a. On this picture the polyp is attached to the haustral fold.

(a)   (b)   (c)
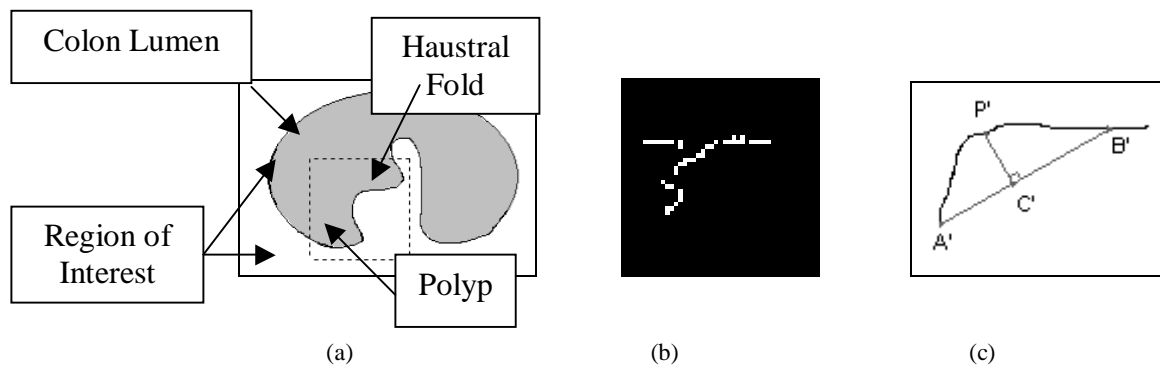
Figure 7. (a) Region of the colon requiring special analysis. (b) Rotated contour image of special case. (c) Diagram shows the beginning of feature extraction

When a polyp edge contour is found in this category our algorithm tries to fit a chord from each pixel to every other edge pixel where the length, best inscribed circle, and height requirements are satisfied. It now becomes possible to continue the feature extraction in the same way except the geometries for locating the polyp apex, and center of inscribed circle are slightly different. Figure 7 shows the rotated edge image and the corresponding diagram detailing the beginnings of feature extraction.

After testing for both polyp types, all images that have been classified as true positive are additionally tested to determine if they are rectal tubes. A small mask is placed in the center of the polyp region *p(x,y)* and an average intensity is calculated. An intensity value less than another given threshold detects air in the center of the "polyp" and corresponds to the center of a rectal tube. This method works because images of rectal tubes processed from CT images are almost always circular and are located easily with our inscribed circle fitting algorithm. If a rectal tube is masquerading as a polyp it will be exposed and not considered for further processing.

The result of segmenting various polyp shapes is quite good and can be seen in figures 8-9 below. The resulting images in the right column are schematic representations of segmentation results. The number of high intensity pixels inside the polyp and the number of polyp edge pixels lying on the inscribed circle are used as features for polyp classification along with radius of inscribed circle, polyp boundary length, polyp height and mean intensity. More features such as polyp base length, intensity standard deviation, skewness and kurtosis (as texture characteristics) could be calculated from the segmentation results and used for more precise classification in the future. Segmentation results could also be presented in more natural form as shown on figure 9.
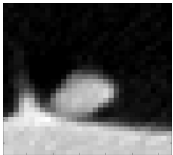
	Original polyp image	Edge Image	Rotated edge image. Polyp and colon walls are gray. Polyp center points are black.	Segmented polyp. High intensity area inside polyp is gray. Polyp edge points close to inscribed circle are shown in black.
1				
2				
3				
4				
5				

Figure 8. Step by step polyp segmentation.

(a)   (b)   (c)   (d)
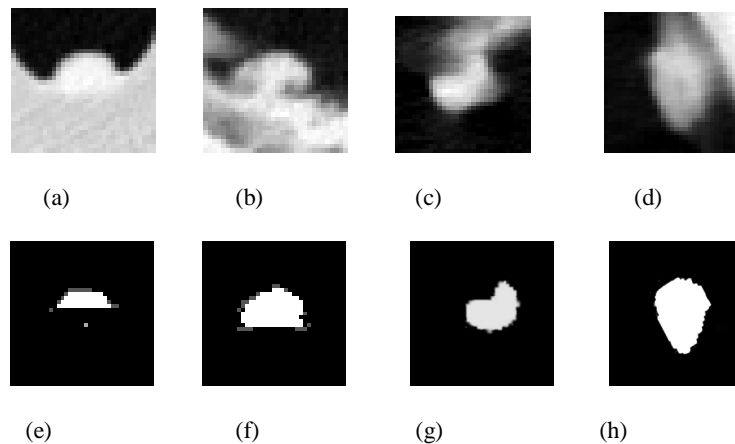

(e)   (f)   (g)   (h)

Figure 9. (a) (b) (c) (d) Original polyp images.
(e) (f) (g) (h) Segmentation results on images rotated along the longest edge line.
Image (h) was rotated back to original image position.

Using the features obtained from the polyp segmentation we developed primitive threshold based classification algorithm. Lower thresholds for the radius of inscribed circle, the number of polyp edge pixels lying on the inscribed circle, the number of high intensity pixels inside the polyp, polyp boundary length, and polyp height are set to eliminate shapes smaller than 3 mm. Upper thresholds are set to remove shapes which are too flat and too big to be a polyp. We are not concerned here about missing very big masses; they are unlikely to be missed by a radiologist, and most of them usually have the smaller bumps on their surfaces, which will be detected by the algorithm. The thresholds for mean intensity aim to eliminate structures with low intensity or intensity higher than tissue, such as leftover stool containing contrast agent, false positive detections caused by streak artifact from metal implants or contrast agent etc.

The threshold based classification was applied to a data set containing 15 polyps larger than 3 mm and 617 false positives taken from 80 CTC studies (supine and prone screening of 40 patients). The sensitivity was 100% (15 of 15). 58% of the FP's were eliminated leaving an average of 3 false positives per study.

3. CONCLUSION

We have developed a CAD algorithm for detecting polyps using CT colonography. As can be seen from the variety of polyp images and results shown above, our method is able to segment polyps and quantitatively measure polyp features independently of orientation and shape. The segmentation algorithm suggested in this paper could also be applied to segment multiple polyp cross-sections obtained from 3D polyp sub-volumes, see for example [5]. More sophisticated classification algorithms such as support vector machine or neural network may be needed to process the results of this segmentation algorithm when it is applied to multiple cross sections taken from 3D polyp sub-volumes.

Based on clinical CTC cases, our algorithm produces 100% sensitivity and only 3 false positives per patient on average. From these results radiologists will only have to interpret a small number of areas in the colon as indicated by our algorithm. Reducing the radiologist's interpretation time translates to cost savings and improvement in the detection of colonic polyps. On a large scale these results are significant due to the number of individuals who are at risk for colon cancer.

4. ACKNOWLEDGMENT

5. REFERENCES

1. O'Brien M, Winawer SJ, Waye JD. Chapter 3. Colorectal polyps. In: S. J. Winawer and R. C. Kurtz, ed. Gastrointestinal cancer. New York: Gower Medical Pub., 1992.
2. M.J. O'Brien, S.J. Winawer, J.D. Waye. Some book on polyps. Get reference from Ron Summers. pg 3.6
3. D.K. Rex, G.A. Lehman, R.H. Hawes, T.M. Ulbright, J.J. Smith, "Screening colonoscopy in asymptomatic average-risk persons with negative fecal occult blood tests," *Gastroenterology,* vol. 100, pp 64-67, 1991.
4. R. M. Summers, C. F. Beaulieu, L. M. Pusanik, J. D. Malley, R. B. Jeffrey, D. I. Glazer, and S. Napel, "Automated polyp detector for CT colonography: Feasibility study," Radiology, vol. 216, no. 1, pp. 284-290, 2000.
5. S. Göktürk, C. Tomasi, B. Acar, C. Beaulieu, D. Paik, and R. Jeffrey, "A statistical 3-D pattern processing method for computer-aided detection of polyps in CT colonography," *IEEE Trans. Med. Imag*., vol. 20(12), pp.1251-60, Dec. 2001.
6. R. Gonzalez and R. Woods, *Digital Image Processing*. Addison Wesley, 1992, pp 198 – 200, pp 414 - 428.
7. R. D. Boyle and R. C. Thomas, *Computer Vision: A First Course*. Blackwell Scientific Publications, 1988, pp 48 - 50.
8. E. R. Davies, *Machine Vision: Theory, Algorithms and Practicalities.* Academic Press, 1990, Chap 5.
9. D. Vernon, *Machine Vision*, Prentice-Hall, 1991, Chap 5.
10. J. Canny, "A Computational Approach to Edge Detection," *IEEE Transactions on Pattern Analysis and Machine Intelligence",* vol. 8, No. 6, pp. 679-698, 1986.
11. R.N. Bracewell, *Two-Dimensional Imaging*. Englewood Cliffs, NJ: Prentice Hall, 1995. pp. 505-537.
12. J.S. Lim, *Two-Dimensional Signal and Image Processing*. Englewood Cliffs, NJ: Prentice Hall, 1990. pp. 42-45.